J Mater Sci (2006) 41:7636–7642
DOI 10.1007/s10853-006-0856-3

Grain size dependence of tensile behavior in nanocrystalline Ni–Fe alloys

Hongqi Li · Fereshteh Ebrahimi · Hahn Choo · Peter K. Liaw

Received: 3 May 2005 / Accepted: 8 November 2005 / Published online: 17 September 2006

Abstract The tensile behaviors of FCC Ni–Fe alloys were investigated within three grain size regimes: >100 nm, 15–100 nm, and <15 nm. The results show that the nanocrystalline metals demonstrated large strain hardening rates, which increase with decreasing the grain size. With the similar grain size, lowing the stacking-fault energy (SFE) by addition of alloying element increases the yield strength and strain hardening ability. The ''low'' tensile elongation of nanocrystalline metals is due to the basic tradeoff between the strength and tensile elongation, i.e. nanostructured metals are not inherently brittle. Both the tensile results and fracture surface observations suggest that the tensile ductility increases with increasing the grain size. Furthermore, within the large grain size regime, the fracture surface exhibited the real void structure; while the fracture surface showed the concave and convex features when the grain size is less than the critical value.

Introduction

For single-phase polycrystals, of various micro-structural variables, grain size plays a significant role in understanding the plastic deformation mechanism, which characteristically determines the mechanical properties. In materials with a grain size of several hundreds nanometers and larger, the deformation is believed to occur by means of the dislocation generation and motion within the grain interior, where the dislocation cells usually form. The increase in the strength with increasing the strain beyond the yield point (i.e., work hardening) arises from the pile-ups and interactions of dislocations. When the grain size is reduced down to a nanocrystalline level (<100 nm), the dislocation activities still prevail [1], whereas grain boundaries act as the sources and sinks of dislocations, and the dislocation entanglements become unlikely because of small crystallite size. The traveling of single dislocations rather than dislocation arrays takes over the deformation [2]. In this case, the stacking-fault energy (SFE) has an important role in the dislocation production due to the dependence of the dislocation splitting distance on the SFE [3]. With a high SFE, i.e., small splitting distance, the perfect dislocations propagate through grain interiors; in contrast, the partial dislocations dominate the intragranular activities in case of a low SFE suggested by computer simulations [4]. With a further decrease in the grain size less than approximately 15 nm, alternative mechanisms, including the grain-boundary mediated activities, govern the plastic deformation [5, 6]. It is, therefore, expected that there exists a transition in the deformation mode from the dislocation to grain-boundary based mechanism with decreasing the grain size below one so called critical value, which has been confirmed by recent studies [4, 7–10]. For face-centered cubic (FCC) metals, this crossover grain size is generally accepted to be about 10–20 nm, depending on the nature of materials.

H. Li (✉) · H. Choo · P. K. Liaw
Department of Materials Science and Engineering, University of Tennessee, Knoxville 37996, USA
e-mail: hqli@utk.edu

F. Ebrahimi
Department of Materials Science and Engineering, University of Florida, Gainesville 32611, USA

For example, it is approximately 12 nm, 14 nm, and 18 nm, respectively, for Ni–Fe alloys [11], copper [7] and aluminum [8]. Note that the transition in the deformation mechanism undergoes gradually because nanocrystals usually have a relatively wide grain size distribution. It is well known that the mechanical properties depend on the deformation mechanism, and, thus, one may anticipate that the mechanical behaviors vary with the grain size. In present study, the uniaxial tensile tests were performed on Ni and Ni–Fe alloys to characterize the effect of the crystallite dimension on tensile behaviors.

Experimental

Four deposits of pure Ni, Ni–6%Fe, Ni–15%Fe and Ni–20%Fe alloys (wt.%) were made via electrodeposition, which is a powerful technique to produce nanostructures. The nanocrystalline and coarse-grained Ni–20%Fe alloys were purchased from Integran and Goodfellow Companies, respectively. The detailed deposition procedures for alloys Ni–6%Fe and Ni–15%Fe can be found elsewhere [12]. The sulfur impurity level in one deposit was analyzed by Wah-Chang company using a LECO CS-444 carbon–sulfur analyzer, which employs the combustion method with infrared detection. Dog-bone shaped specimens were used for tensile tests at a nominal strain rate of 10^{-4} s^{-1} at room temperature. Microstructural analysis and fracture surface examinations were conducted using transmission electron microscopy (TEM) and scanning electron microscopy (SEM).

Results and discussion

Microstructure

The composition analysis was applied using a JEOL 733 Electron Microprobe (EMP), with an accuracy of 1% (wt.%). The results show that the compositional distribution of the electrodeposited Ni–Fe alloys is quite homogeneous throughout the whole deposit. The impurity such as sulfur in the deposits was measured to be less than 100 ppm (parts per million by weight). X-ray diffraction analysis further reveals that the Ni–Fe alloys used have a single FCC phase, indicative of a complete solid solution of Fe into Ni.

The dark field TEM pictures of pure Ni, Ni–6%Fe, Ni–15%Fe, and Ni–20%Fe alloys as well as their grain size distributions are given in Fig. 1. The results demonstrate that the grain size distributions of the Ni–15%Fe and Ni–20%Fe alloys are much narrower than those for the low iron alloy and pure Ni, which is due to the addition of the alloying element [12]. For example, the grain size ranges are 3–30 nm and 5–50 nm for the Ni–15%Fe and Ni–20%Fe alloys, respectively. However, the pure Ni and Ni–6%Fe alloy have quite wide grain size distributions of 5–155 nm and 5–305 nm, correspondingly. According to the measurement on hundreds of grains and their relative number frequencies, the calculated mean grain sizes are approximately 44 nm, 53 nm, 21 nm, and 9 nm, respectively, for pure Ni, Ni–6%Fe, Ni–20%Fe, and Ni–15%Fe alloys. The coarse-grained Ni–20%Fe alloy from Goodfellow Company has a grain size of about 35 μm. For Ni and Ni–Fe alloys, on the basis of the hardness and tensile results, the critical grain size is approximately 8–12 nm [11, 13]. Therefore, the nanostructured pure Ni, Ni–6%Fe, Ni–20%Fe and coarse grained Ni–20%Fe alloys fall into the large grain size range, i.e., larger than the critical grain size for these materials, and the Ni–15%Fe alloy is among the small grain size regime, i.e., smaller than the critical grain size for this material.

The characteristics of grain boundaries in nanocrystalline deposits were studied using high resolution TEM. Figure 2 presents examples of the grain boundary structure in the deposit of Ni–15%Fe. Figure 2a illustrates an example of high-angle grain boundary between grains 1 and 2. It is clear that the grain boundary is atomistically sharp and the crystallinity is maintained up to the boundary, indicating that no second phases formed at grain boundaries. In addition to the prevalent high-angle boundaries, the low-angle grain boundary was occasionally detected, as seen in Fig. 2b, where four dislocations (black ⊥) array along the grain boundary of grains 3 and 4.

Tensile results

Figure 3a shows the engineering stress–strain curves of these five materials. In general, the strengths of all four nanocrystalline metals are several times higher than their coarse-grained counterparts. For example, the yield strength of nanocrystalline Ni–20%Fe (21 nm) was measured at about 1500 MPa, while it is only 190 MPa for its microcrystalline counterpart. More importantly, a comparison of the curves between pure nickel (44 nm) and the Ni–6%Fe alloy (53 nm) reveals that in spite of the larger grain size of the alloy, it exhibited the higher yield strength than pure Ni did. The increase in the strength due to the addition of iron is associated with the substitutional solid solution

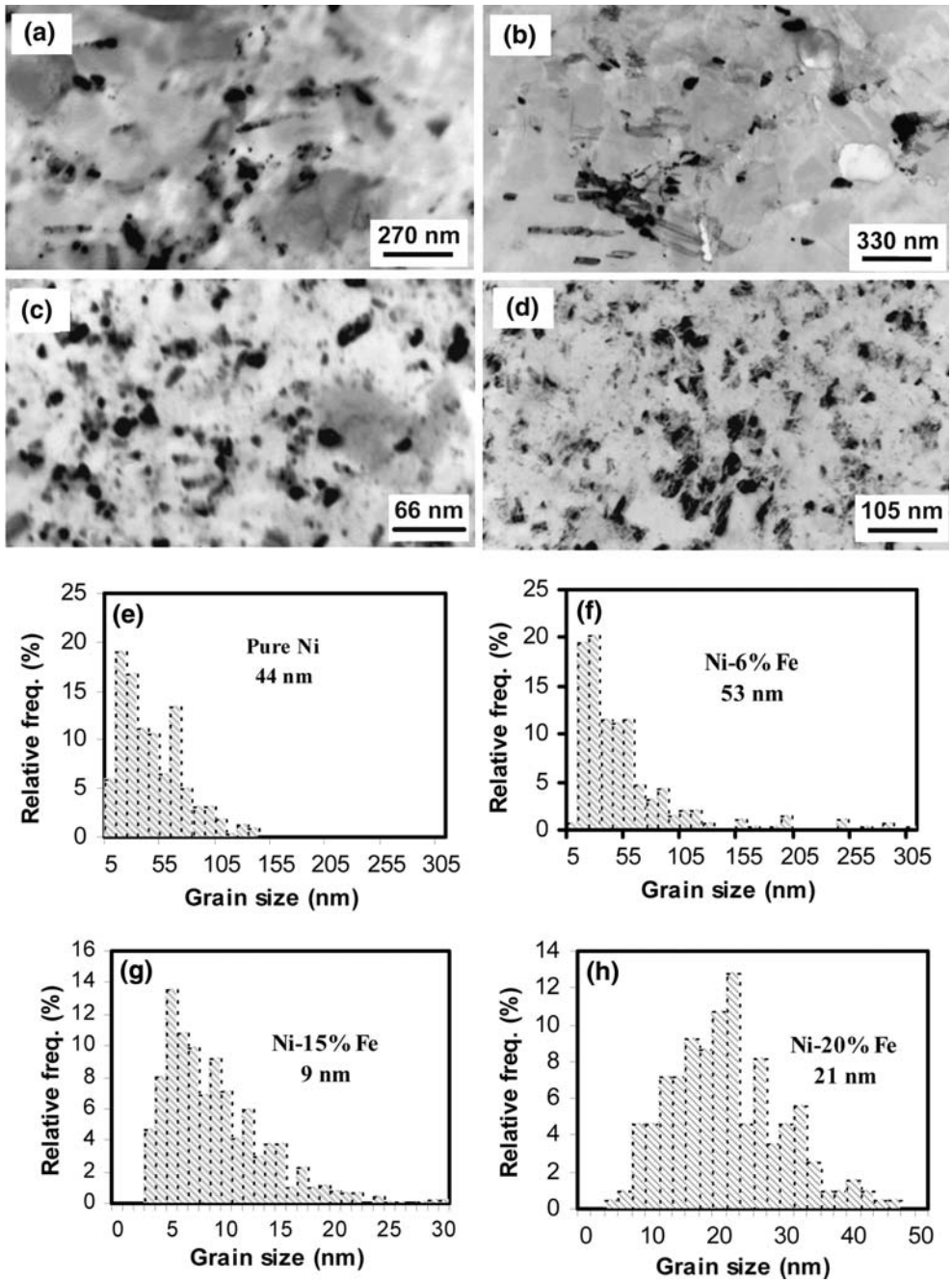

Fig. 1 Dark-field TEM images of (**a**) pure Ni, (**b**) Ni–6%Fe, (**c**) Ni–15%Fe and (**d**) Ni–20%Fe alloys. (**e**–**h**) presenting their corresponding grain size distributions

hardening mechanism. On the other hand, the reduction of the SFE may also plays a role in that the first emitted partials can block the generation of the later stacking faults in the low SFE materials [4]. For nanocrystalline Ni–15%Fe and Ni–20%Fe alloys, their high strength could be attributed to both the small grain size and the alloying element. Note that the lack of inverse Hall–Petch relationship in the strength is because the Ni–15%Fe alloy (9 nm) is much closer to the critical grain size (8–12 nm) than Ni–20%Fe (21 nm) alloy does. Current nanostructured metals had a tensile elongation of more than 5%, which is a remarkable improvement in contrast to the reported data regarding the electrodeposited nanocrystals [13–15]. Typically, there exists a fundamental tradeoff between the strength and the tensile elongation for any materials [16], as shown in Fig. 3b, where the data of copper, nickel and conventional Permalloy are from references of [17], [14] and [18], respectively. According to this tradeoff, the tensile elongation of more than 5% in nanocrystalline Ni and Ni–Fe alloys is acceptable at such high strength level. Recent results

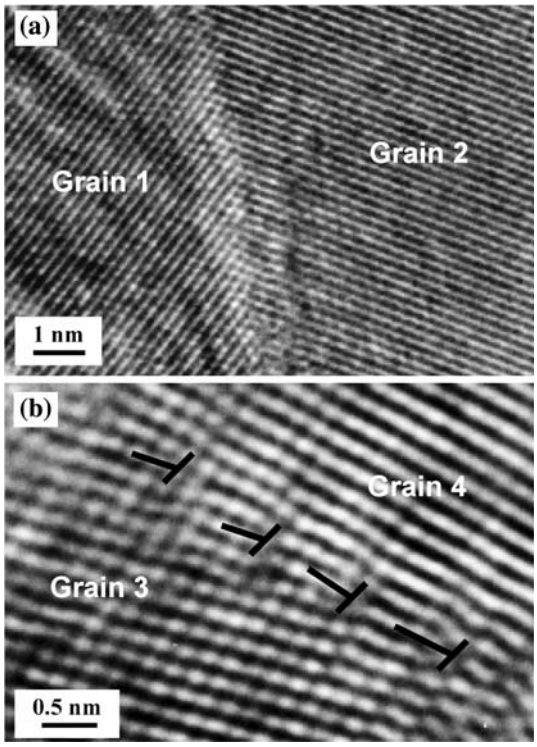

Fig. 2 High resolution TEM images showing (**a**) high angle and (**b**) low angle grain boundaries in the Ni–15%Fe alloy. Each back ⊥ denotes one dislocation

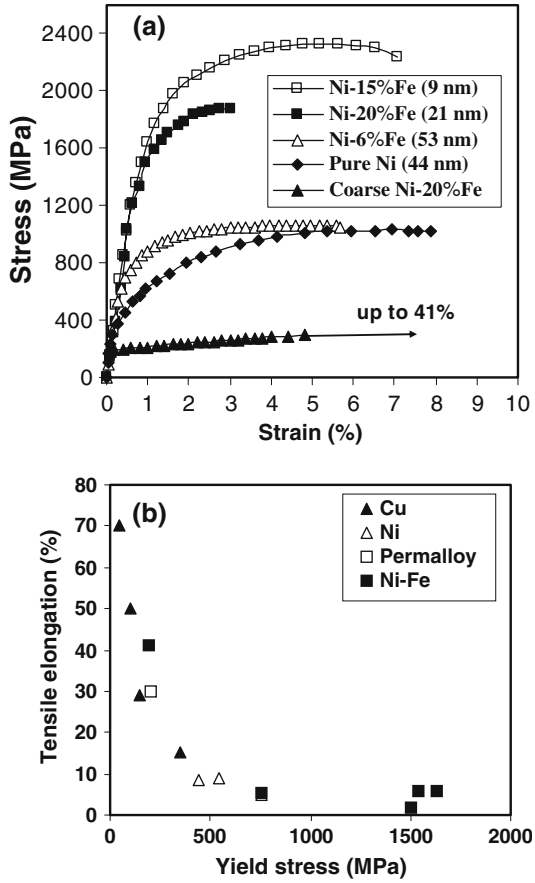

Fig. 3 (**a**) Tensile engineering stress–strain curves of all the five specimens and (**b**) plastic tensile elongation at failure-yield stress curve

reported that the plastic deformation could cause grain growth in nanocrystalline pure Cu [19]. The grain growth is probably associated with the severe plastic deformation, for instance, in case of compression. However, no such phenomena were found in the samples presently studied. The reasons for this discrepancy are still not clear. The lack of grain growth in current study is probably due to the low plastic deformation in case of tension.

The initial strain hardening rate–true strain curves are plotted in Fig. 4. It is clear that the nanocrystalline metals strain hardened largely stronger than the conventional Ni–20%Fe alloy did at the early stage of the plastic deformation. In general, the smaller the grain size, the larger the strain hardening rate. Interestingly, for nanocrystalline Ni and Ni–6%Fe alloy, although the alloy has larger grain size, their strain hardening rates are similar. This finding confirms the recent computer simulation results that the decrease in the SFE leads to the increase in the strain hardening ability [4, 20]. It can be expected that with the similar grain size, the alloys would have higher strain hardening rate than pure metals. In case of Ni–15%Fe and Ni–20%Fe alloys, the effect of the SFE on the strain hardening rate is covered by the remarkable difference in their grain sizes (the grain size of the Ni–20%Fe alloy is more than two times larger than that of the Ni–15%Fe alloy). In coarse grained metals, the strain hardening is caused by the interaction of dislocations and dislocation pile-ups at grain boundaries within grains.

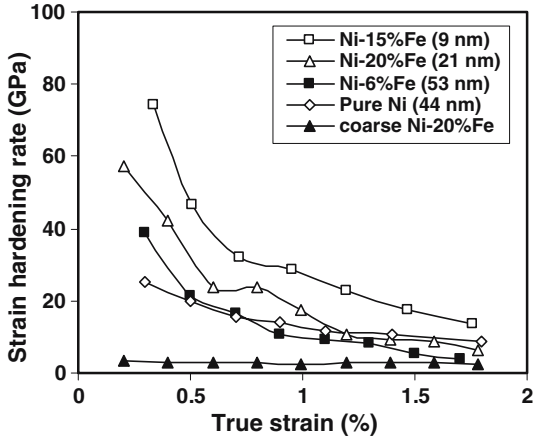

Fig. 4 Strain hardening rate–true strain curves of all the five samples

According to computer simulation results [7, 8], at the nano scale, the plastic deformation proceeds with individual dislocation motion and/or grain boundary activities. As a result, the dislocation entanglements inside grains becomes less or impossible, which has been verified by the synchrotron diffraction study on the nanocrystalline Ni [21]. At such situation, the strain hardening is no longer caused by the interaction of dislocations and is suggested to originate from the intergranular stresses that develop owing to the strain incompatibility among various grains, which is similar to the deformation mechanism of a composite [22]. That is, the level of the plastic strain varies among grains with different diameters, and at a given stress level, there exist a fraction of grains, which deform only elastically [22, 23]. The reduction of the internal stress and the decrease in the volume fraction of elastic grains result in the decrease of the strain hardening rate [22]. The relief of the local internal stress can be realized by dislocation and grain boundary activities. At different grain sizes, the significance of these two components is different. At large grain sizes, the decreasing in the strain hardening rate with increasing strain is mainly due to the recovery processes associated with the cross-slip and climb of dislocations. However, at small grain sizes, the decrease in the rate of strain hardening with strain is attributed to an increase in the extent of grain boundary activities because the degree of the grain boundary deformation increases with increasing the applied strain [7].

Fractography

Figure 5 presents the SEM observations on the fracture surfaces. Because the fracture features of pure Ni and Ni–20%Fe alloy are similar to those for Ni–6%Fe alloy, their images are not shown here. It is found that the coarse-grained samples demonstrated necking in both width and thickness directions, whereas the necking took place only along the thickness direction in case of nanocrystalline specimens due to the thin cross-section of these samples. At low magnifications, the estimated reductions in area, an indicator of ductility, are about 55%, 80%, and less than 5% for the microcrystalline Ni–20%Fe, nanocrystalline Ni–6%Fe, and Ni–15%Fe alloys, respectively. For the coarse-grained Ni–20%Fe and nano-grained Ni–15%Fe alloys, there is a correlation between the tensile elongation and reduction of area in these samples. However, it is of interest that the Ni–6%Fe alloy exhibited a severe necking behavior, indicating the extensive localized deformation. Sometimes, the fracture surface

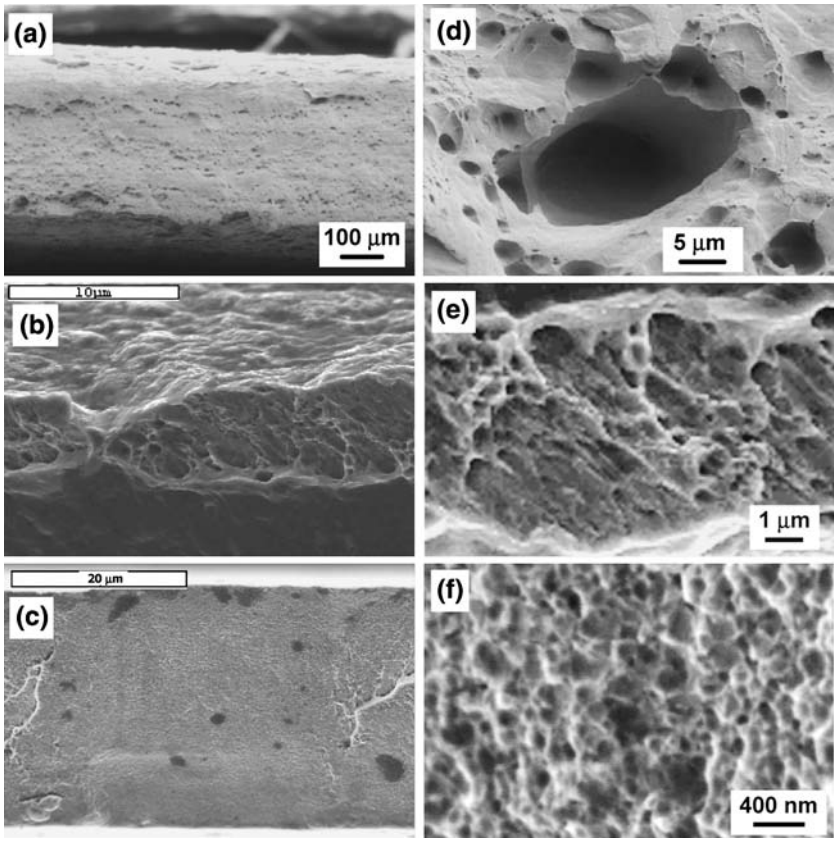

Fig. 5 SEM micrographs of fracture surfaces at low and high magnifications: (**a**) and (**d**) coarse-grained Ni–20%Fe, (**b**) and (**e**) Ni–6%Fe, and (**c**) and (**f**) Ni–15%Fe alloys

shows a knife-edge phenomenon [14]. The mechanism responsible for such behavior is still not well established. At high magnifications, all the three materials exhibited the microvoid structure on their fracture surfaces. Detailed analysis revealed that, in case of nanostructured alloys, the void size has a scale of several times of the grain size value, suggesting that every void covers many grains; while the voids are usually smaller than the grain size in coarse-grained Ni–20%Fe alloy. In addition, it is also disclosed that the void size distribution becomes more uniform with decreasing the grain size. Furthermore, it is worthwhile that the void depth increases with an increase in the grain size, meaning that the ductility rises with increasing the grain size. It is widely known that microvoids form by the initiation, growth, and coalescence processes for the conventional FCC metals. For the Ni–6%Fe alloy, the TEM study suggests that the void initiation usually occurs at the grain boundaries and triple junctions [1]. The microvoid growth mechanism is believed to be the same as that in coarse-grained FCC metals and, the coalescence is caused by breaking the ligaments between voids. However, in case of the Ni–15%Fe alloy with a grain size of less than the critical value, it is suggested by computer simulation that the microvoid formation is accomplished by the development of shear planes around a group of grains [24]. The final failure occurs by way of breaking the atomic bonds at grain boundaries along these shear planes, indicating an intergranular fracture mode, as shown in Fig. 6, in which the crack propagated along grain boundaries. It is worth noting that no microvoid coalescence takes place in such a case, and the microvoid size is determined by the size of clusters included by the shear planes. Figure 5d, e show that for coarse-grained Ni–20%Fe and nanocrystalline Ni–6%Fe alloys all the microvoids have the concave features on the fracture surfaces, indicating a typical void characteristic. However, in case of nano-grained Ni–15%Fe alloy, detailed examination discloses that both the concave (void) and convex (cone) features exist on the fracture surface, as seen in Fig. 7, where the black and white arrows indicate the convex and concave characteristics, respectively. These differences are associated with the different deformation mechanisms at different grain sizes.

Figure 8 illustrates the representative SEM images of side surfaces. It is obvious that many deformation bands were observed within the area close to the fracture surface, and no such bands were detected far away from the

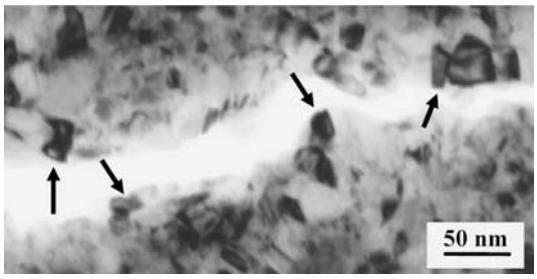

Fig. 6 Bright-field TEM image of nanocrystalline Ni–15%Fe alloy shows intergranular fracture along grain boundaries indicated by black arrows

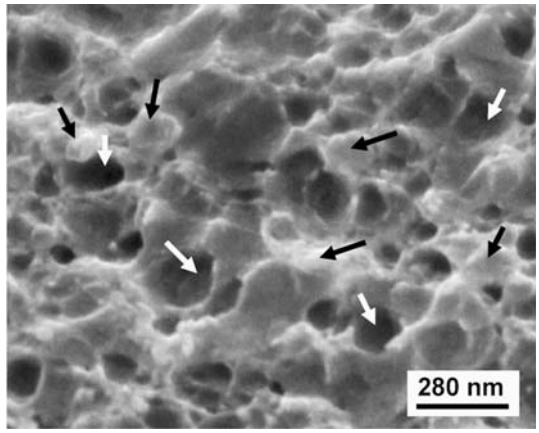

Fig. 7 SEM picture of nanocrystalline Ni–15%Fe alloy's fracture surface. The black and white arrows identify the convex and concave features, respectively

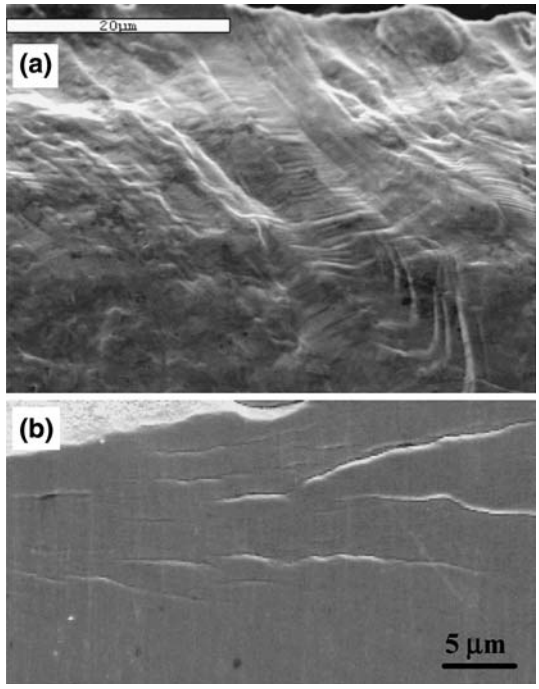

Fig. 8 SEM observations near the fracture surface: (**a**) Ni–6%Fe, and (**b**) Ni–15%Fe alloys

fracture surface for the Ni–6%Fe alloy, demonstrating the considerable localized deformation within the necked region. However, in the case of Ni–15%Fe alloy, aside from the deformation bands, there exist a great number of microcracks near the fracture surface, as shown in Fig. 8b. Note that no microcracks were found in the pure Ni, Ni–6%Fe, Ni–20%Fe and coarse-grained Ni–20%Fe alloys. These findings again suggest that the ductility increases with increasing the grain size, which is in good agreement with the tensile results and the fracture surface observations.

Conclusion

The nanocrystalline pure Ni and Ni–Fe alloys were fabricated using an electrodeposition technique. The tensile behaviors of Ni and Ni–Fe alloys were studies at different grain sizes: larger than 100 nm, 15–100 nm, and less than 15 nm. The results demonstrate that there is a trade-off between the yield strength and tensile elongation, and the nano metals are not intrinsically brittle. In addition, the nano-grained metals strain-harden significantly rapidly in comparison with the micro-grained ones. The strain hardening rate depends on both the grain size and the SFE. In all situations, the fracture surfaces were featured by microvoid characteristics. However, both the void size and depth increase with increasing the grain size, whereas the microvoid size distribution becomes more homogeneous with decreasing the grain size. Detailed analysis reveals that, at larger grain sizes, the microvoids on the fracture surface are real concave voids and the fracture takes place in an intragranular manner; while at small grain size, the fracture surface exhibits both the concave and convex features and the fracture model is intergranular. As a summary of the current study, based on the tensile properties and the fracture behaviors, it can be concluded that the tensile ductility increases with increasing the grain size.

Acknowledgements This work was supported by the National Science Foundation (NSF) under the grant # DMR-9980213 at Materials Science and Engineering Department of the University of Florida and DMR-0231320 at Materials Science and Engineering Department of the University of Tennessee.

References

1. Kumar KS, Suresh S, Chisholm MF, Horton JA, Wang P (2003) Acta Mater 51:387
2. Embury JD, Hirth JP (1994) Acta Metall Mater 42:2051
3. Dieter GE (1986) Mechanical metallurgy. McGraw-Hill, New York, p 168
4. Yamakov V, Wolf D, Phillpot SR, Mukherjee AK, Gleiter H (2004) Nat Mater 3:43
5. Schiøtz J, Di Tolla FD, Jacobsen KW (1998) Nature 391:561
6. Van Swygenhoven H (2002) Science 296:66
7. Schiøtz J, Jacobsen KW (2003) Science 301:1357
8. Yamakov V, Wolf D, Phillpot SR, Mukherjee AK, Gleiter H (2003) Phil Mag Lett 83:385
9. Liao XZ, Zhao YH, Zhu YT, Valiev RZ, Gunderov DV (2004) J Appl Phys 96:636
10. Nieh TG, Wadsworth J (1991) Scripta Met Mater 25:955
11. Cheung C, Palumbo G, Erb U (1994) Scripta Met Mater 31:735
12. Li H, Ebrahimi F (2003) Mater Sci Eng A 347:93
13. Wang N, Wang Z, Aust KT, Erb U (1997) Mater Sci Eng A 237:150
14. Ebrahimi F, Bourne GR, Kelly MS, Matthews TE (1999) NanoStruct Mater 11:343
15. Legros M, Elliott BR, Rittner MN, Weertman JR, Hemker KJ (2000) Philos Mag A 80:1017
16. Matlock DK, Zia-Ebrahimi F, Krauss G (1984) In: Krauss G (ed) Deformation, processing and structure. ASM Publication, Metals Park, Ohio, p. 47
17. Valiev RZ, Alexandrov IV, Zhu YT, Lowe TC (2002) J Mater Res 17:5
18. McCrea JL, Palumbo G, Hibbard GD, Erb U (2003) Rev Adv Mater Sci 5:252
19. Zhang K, Weertman JR, Eastman JA (2005) Appl Phys Lett 87:061921
20. Yip S (2004) Nature Mater 3:11
21. Budrovic Z, Van Swygenhoven H, Derlet PM, Van Petegem S, Schmitt B (2004) Science 304:273
22. Ebrahimi F, Ahmed Z, Morgan KL (2001) MRS Symp Proc 634:B2.7.1
23. Mitra R, Ungar T, Morita T, Sanders PG, Weertman JR (1999) In: Chung Y-W, Dund DC, Liaw PK, Olsen GB (eds) The 1999 J.R. Weertman Symposium. TMS, Warrendale, PA, p 553
24. Hasnaoui A, Van Swygenhoven H, Derlet PM (2003) Science 300:1550